



*Institute of Paper Science and Technology
Atlanta, Georgia*

IPST Technical Paper Series Number 852

Scale-Dependent Bounds on Effective Elastoplastic
Response of Random Composites

M. Jiang, M. Ostoj-Starzewski, and I. Jasiuk

May 2000

Submitted to
Journal of the Mechanics and Physics of Solids

Copyright© 2000 by the Institute of Paper Science and Technology

For Members Only

INSTITUTE OF PAPER SCIENCE AND TECHNOLOGY PURPOSE AND MISSIONS

The Institute of Paper Science and Technology is an independent graduate school, research organization, and information center for science and technology mainly concerned with manufacture and uses of pulp, paper, paperboard, and other forest products and byproducts. Established in 1929 as the Institute of Paper Chemistry, the Institute provides research and information services to the wood, fiber, and allied industries in a unique partnership between education and business. The Institute is supported by 52 North American companies. The purpose of the Institute is fulfilled through four missions, which are:

- to provide multidisciplinary graduate education to students who advance the science and technology of the industry and who rise into leadership positions within the industry;
- to conduct and foster research that creates knowledge to satisfy the technological needs of the industry;
- to provide the information, expertise, and interactive learning that enables customers to improve job knowledge and business performance;
- to aggressively seek out technological opportunities and facilitate the transfer and implementation of those technologies in collaboration with industry partners.

ACCREDITATION

The Institute of Paper Science and Technology is accredited by the Commission on Colleges of the Southern Association of Colleges and Schools to award the Master of Science and Doctor of Philosophy degrees.

NOTICE AND DISCLAIMER

The Institute of Paper Science and Technology (IPST) has provided a high standard of professional service and has put forth its best efforts within the time and funds available for this project. The information and conclusions are advisory and are intended only for internal use by any company who may receive this report. Each company must decide for itself the best approach to solving any problems it may have and how, or whether, this reported information should be considered in its approach.

IPST does not recommend particular products, procedures, materials, or service. These are included only in the interest of completeness within a laboratory context and budgetary constraint. Actual products, materials, and services used may differ and are peculiar to the operations of each company.

In no event shall IPST or its employees and agents have any obligation or liability for damages including, but not limited to, consequential damages arising out of or in connection with any company's use of or inability to use the reported information. IPST provides no warranty or guaranty of results.

The Institute of Paper Science and Technology assures equal opportunity to all qualified persons without regard to race, color, religion, sex, national origin, age, disability, marital status, or Vietnam era veterans status in the admission to, participation in, treatment of, or employment in the programs and activities which the Institute operates.

**SCALE-DEPENDENT BOUNDS ON EFFECTIVE ELASTOPLASTIC
RESPONSE OF RANDOM COMPOSITES**

M. Jiang¹, M. Ostoja-Starzewski^{2*}, and I. Jasiuk¹

¹The George W. Woodruff School of Mechanical Engineering
Georgia Institute of Technology
Atlanta, GA 30332-0405, USA

²Institute of Paper Science and Technology, and Georgia Institute of Technology
500 10th Street, N.W.
Atlanta, GA 30318-5794, USA

To be published in
Journal of the Mechanics and Physics of Solids

* corresponding author; e-mail: martin.ostoja@ipst.edu

ABSTRACT

We consider the mechanical response of random, heterogeneous materials, where each phase is elastic-plastic with an associated flow rule, and the microstructure's statistics is homogeneous and ergodic. Under proportional monotonic loading, the effective (in the macroscopic sense, or overall) elastoplastic response is shown to be bounded from above and below by those obtained, respectively, from displacement and traction boundary conditions applied to finite size domains (square shaped windows). A scale dependent hierarchy of these bounds is obtained by extending the methods used earlier for the elastic moduli estimation: the larger the scale relative to the heterogeneity, the closer are the bounds. A fiber reinforced metal matrix composite is employed to illustrate the theoretical results. Its constitutive response and plastic strain field are investigated by computational micromechanics for different window sizes under both types of boundary conditions; it is found here that the displacement conditions result in denser and more uniformly distributed slip band patterns, while the traction conditions lead to more localized fields. We also investigate a mixed boundary condition, under which the mechanical response of composite is found to fall between those under displacement and traction controlled boundary conditions.

Key words: *scale and boundary conditions effects; B: fiber-reinforced composite material; C. energy methods; finite elements; probability and statistics*

1. INTRODUCTION

The subject of effective (in the macroscopic sense, or overall) response of elastoplastic composites dates back to Sachs (1928) and Taylor (1938). However, it came into focus of extensive studies in the eighties and nineties – this was made possible by the groundwork laid by the progress of micromechanics of elastic materials and the advancement of computational mechanics. Thus, all the works can, basically, be classified in three categories: (i) rigorous bounds on the effective response, (ii) effective medium estimates, and (iii) computational mechanics models.

In the first category, we mention the works of Accorsi and Nemat-Nasser (1986) and Teply and Dvorak (1988) on bounds of instantaneous elastoplastic moduli for composites with periodic microstructures. The subsequent progress for more general composites is illustrated by the studies of Ponte Castañeda (1992) and, most recently, by Talbot and Willis (1998), for example. An excellent review of various methods was given by Ponte Castañeda and Suquet (1998). The works in the second category are exemplified by Li and Ponte Castañeda (1994); see also references therein. Studies in the third category focused on the effective response of periodic and disordered microstructures, e.g., (Brockenbrough *et al.*, 1991; Moulinec and Suquet, 1994, 1998). Various other interesting results were obtained on the effects of shape of inclusions (Shen *et al.*, 1995), and random fiber arrangement geometries (Werwer *et al.*, 1998).

Clearly, all these research categories are, in a following sense, mutually complementary: the first one studies bounds on response of the RVE, while the second and third obtain quantitative results on the actual RVE, oftentimes under a restrictive assumption of spatial periodicity of the composite material. By the RVE we mean here the so-called Representative Volume Element of continuum mechanics. Indeed, the RVE concept in the sense of Hill (1963)

is the motivation of the present work. Namely, we want to investigate the effects of scale and boundary conditions for domains of the material finite relative to the size of the heterogeneity, and thereby to assess the approach to the RVE.

Our strategy in finding the scale-dependent bounds on the elastoplastic constitutive response is analogous to that employed for the linear elastic case (Huet, 1990; Sab, 1992; Ostoj-Starzewski, 1993). The main idea is to employ the boundary conditions and the extremum principles. It can then be shown that, under proportional monotonic loading, the elastoplastic responses under displacement and traction boundary conditions provide scale dependent upper and lower bounds, respectively, for the true effective elastoplastic response. As a result, the larger the scale of the test domain (called a window) relative to the heterogeneity, the closer are the bounds. A fiber reinforced metal matrix composite is employed to illustrate the theoretical results. Its constitutive responses and plastic strain fields in shear tests are investigated by computational micromechanics for different window sizes under various types of boundary conditions – displacement, traction and mixed. However, the determination of the yield function is beyond the scope of this paper.

2. PROBLEM FORMULATION

We consider composite materials characterized by one microscale, such as the diameter d of inclusions; fractal geometries are excluded. All the fibers are aligned, so that our problem is one of plane strain in the transverse x_1, x_2 -plane. In principle, any sample of the composite is disordered but not random - it represents a deterministic realization $B(\omega)$ of a random medium $B = \{ B(\omega); \omega \in \Omega \}$, where Ω is a sample space. In order to generate a field of round disks (fiber sections), we employ a Poisson point process for the disk centers subject to a sequential

inhibition rule: throw Poisson points onto a plane and keep only those which fall no closer than $1.1 \cdot d$ to any previous ones. This condition prevents the touching of disks, so as to obviate, in our computational mechanics study, the problem of very narrow necks between disks.

Any realization $B(\omega)$ of the composite \mathbf{B} (set of all $B(\omega)$'s) is, in the first place, described by a characteristic function $\chi_p(\mathbf{x}, \omega)$ taking the value 1 in the region occupied by material of type p and 0 elsewhere. The constitutive response of each phase $p (= 1, \dots, p_{tot})$ is elastic-plastic-hardening with the plastic regime following the associated flow rule (Hill, 1983)

$$\begin{aligned}
 d\varepsilon_{ij}' &= \frac{d\sigma_{ij}'}{2G_p} + \lambda \frac{\partial f_p}{\partial \sigma_{ij}} df_p \quad \text{whenever} \quad f_p = c_p \quad \text{and} \quad df_p \geq 0 \\
 d\varepsilon_{ij}' &= \frac{d\sigma_{ij}'}{2G_p} \quad \text{whenever} \quad f_p < c_p \\
 d\varepsilon &= \frac{1-2\nu_p}{2G_p(1+\nu_p)} d\sigma \quad \text{everywhere} \quad (d\varepsilon = d\varepsilon_{ii}/3, d\sigma = d\sigma_{ii}/3)
 \end{aligned} \tag{2.1}$$

where primes indicate deviatoric tensor components, and there is no summation over p . Thus, G_p , ν_p and c_p form a vector $\Theta_p = \{G_p, \nu_p, c_p\}$, whose each component gives rise to a random field, such as

$$G(\mathbf{x}, \omega) = \sum_{p=1}^{p_{tot}} G_p \chi_p(\mathbf{x}, \omega), \quad \omega \in \Omega \tag{2.2}$$

All together, we have a random field $\Theta = \{G, \nu, c\}$. The Poisson point process for the disk centers is homogeneous (invariant with respect to arbitrary shifts in the x_1, x_2 -plane), and has a mixing property, which is known to be a sufficient condition for it to be ergodic (Stoyan *et al.*, 1987). As a result, the vector-valued random field $\Theta = \{G, \nu, c\}$, is homogeneous and ergodic, too.

We want to ascertain the overall properties of the composite material in a *window* of size L , such as those shown in Fig. 1. Of course, windows of size $L \rightarrow \infty$ yield the pointwise limit of local properties, while windows of finite size define a scale over which some ‘smearing out’ is conducted. In the following we shall study this smearing out as a function of a nondimensional window scale

$$\delta = \frac{L}{d} \quad (2.3)$$

and, following Huet (1990), shall call the window’s properties *apparent*, rather than *effective*. The latter adjective is reserved for the $\delta \rightarrow \infty$ limit, in which, given the statistical homogeneity and ergodicity of the material, the response for every specimen $B(\omega)$ of a random medium \mathbf{B} should be identical. Of course, when considering finite δ values, the response is not deterministic, so that the window represents a mesoscale Statistical Volume Element (SVE). The limit $L/d \rightarrow \infty$ in (2.3) is understood in the sense of the homogenization theory (e.g., Sanchez-Palencia & Zaoui, 1987; Sab, 1992): $\mathbf{x} \rightarrow \mathbf{G}(\mathbf{x}) = \mathbf{G}(\mathbf{x}/\varepsilon) \equiv \mathbf{G}(\mathbf{y})$, where \mathbf{x} and \mathbf{y} are the so-called slow (macroscopic) and fast (microscopic) variables, and ε is a small parameter, reciprocal of our $\delta = L/d$ (in the sections that follow ε denotes strain). This limiting process is schematically illustrated by a sequence of (a) and (b) in Fig.1.

3. HIERARCHY OF BOUNDS

It is well known that, for linear elastic heterogeneous materials, all the necessary and sufficient conditions of the equivalence between the energetically and mechanically defined effective properties of elastic materials are contained in the so-called Hill condition (Hill, 1963)

$$\overline{\boldsymbol{\sigma} : \boldsymbol{\varepsilon}} = \overline{\boldsymbol{\sigma}} : \overline{\boldsymbol{\varepsilon}} \quad (3.1)$$

This condition means that the average of the product of the stress and strain tensors equals the product of their averages. In this paper, we use bar over a quantity to denote its volume average and reserve $\langle \rangle$ to denote its ensemble average. It was shown by Huet (1981, 1982, 1984, 1990) that for an unbounded space domain, (3.1) is trivial, but for a finite body it imposes important restrictions on the boundary conditions.

Recently, Hazanov (1998) generalized (3.1) to nonlinear heterogeneous materials, and for a static case, there is

$$\overline{\int \sigma : d\varepsilon} = \int \bar{\sigma} : d\bar{\varepsilon} \quad \Leftrightarrow \quad \int_{\partial B_\delta} (t - \bar{\sigma} \cdot n) \cdot d(u - \bar{\varepsilon} \cdot x) dS = 0 \quad (3.2)$$

where ∂B_δ is the boundary of a given window B_δ of size δ . From (3.2), one can obtain three kinds of boundary conditions. They are

(i) kinematic uniform boundary condition (or displacement controlled boundary condition)

$$u = \bar{\varepsilon} \cdot x, \quad \forall x \in \partial B_\delta \quad (3.3)$$

(ii) static uniform boundary condition (or traction controlled boundary condition)

$$t = \bar{\sigma} \cdot n, \quad \forall x \in \partial B_\delta \quad (3.4)$$

(iii) mixed uniform boundary condition

$$(t - \bar{\sigma} \cdot n) \cdot (u - \bar{\varepsilon} \cdot x) = 0, \quad \forall x \in \partial B_\delta \quad (3.5)$$

It is known that, under proportional monotonic loading, effectively, strain-hardening elastoplastic composites can be treated in the framework of deformation theory, which is formally equivalent to physically nonlinear, small-deformation elasticity. We assume that this equivalence also holds for apparent elastoplastic response, and in the following, we study the apparent properties for generally nonlinear elastic composites. The results obtained can be used

in apparently elastoplastic response analysis of a composite whose phases behave in a strain-hardening way.

Taking all the phases of the composite as nonlinear elastic, the constitutive behavior of any individual phase is governed by a strain-energy function $w(\epsilon)$, so that (Ponte Castañeda and Suquet, 1998; Willis and Talbot, 1990)

$$\sigma = \frac{\partial w(\epsilon)}{\partial \epsilon} \quad (3.6)$$

Corresponding to w , there is a complementary energy density function w^*

$$w^* = \sigma : \epsilon - w \quad (3.7)$$

such that

$$\epsilon = \frac{\partial w^*(\sigma)}{\partial \sigma} \quad (3.8)$$

The functions w and w^* are dual potentials.

The following proof procedure is similar to that by Huet (1990). Consider a partition of the window $B_\delta(\omega)$ of scale δ into n^2 smaller square-shaped sub-windows B_δ^s , $s = 1, 2, \dots, n^2$, of sizes $\delta^s = \delta/n$. We define two types of boundary conditions, in terms of a prescribed strain ϵ^0 , over the large window with any given microstructure $B_\delta(\omega) = \cup_{s=1}^{n^2} B_\delta^s(\omega)$: unrestricted

$$u_i = \epsilon_{ij}^0 x_j, \quad x \in \partial B_\delta \quad (3.9)$$

and: restricted

$$u_i^r = \epsilon_{ij}^0 x_j, \quad x \in \partial B_\delta^s, \quad s = 1, 2, \dots, n^2 \quad (3.10)$$

Superscript r in (3.10) indicates a ‘restriction’. The classical minimum theorem of the potential energy for elasticity without volume forces states that, among the set $\{\tilde{\varepsilon}, \tilde{u}\}$ of all admissible solutions, the functional

$$\Pi(\tilde{\varepsilon}) = \int w(\tilde{\varepsilon}_{ij})dV - \int_{\partial B_{\delta}^t} t_i u_i dS \quad (3.11)$$

is a minimum for the true solution (ε, u) , where ∂B_{δ}^t stands for that part of ∂B_{δ} on which the traction vector t is prescribed.

In general, we have, for any body

$$\partial B_{\delta} = \partial B_{\delta}^d \cup \partial B_{\delta}^t \quad (3.12)$$

where ∂B_{δ}^d is that part of ∂B_{δ} on which the displacements are prescribed.

Because under (3.9) and (3.10) $\partial B_{\delta} = \partial B_{\delta}^d$ and $\partial B_{\delta}^t = \emptyset$, the potential energies $\Pi(\omega)$ and $\Pi^r(\omega)$ (i.e., unrestricted versus restricted conditions) stored in B_{δ} are

$$\Pi(\omega) = W(\omega; \varepsilon^0) \quad \text{and} \quad \Pi^r(\omega) = W^r(\omega; \varepsilon^0) \quad (3.13)$$

where

$$W(\omega; \varepsilon^0) = \int w dV \quad \text{and} \quad W^r(\omega; \varepsilon^0) = \int w^r dV \quad (3.14)$$

In view of the principle of minimum potential energy, the following inequality holds

$$W(\omega; \varepsilon^0) \leq W^r(\omega; \varepsilon^0) \quad (3.15)$$

If we denote $W(\varepsilon^0, \delta)$ as the strain energy of an RVE with partitioning by windows of size δ under displacement controlled boundary condition, then from (3.15) we have

$$W(\varepsilon^0, \Delta) \leq W(\varepsilon^0, \delta) \leq W(\varepsilon^0, \delta') \leq W(\varepsilon^0, I) \equiv W^V \quad \text{for} \quad I < \delta' < \delta < \Delta \quad (3.16)$$

where Δ is the RVE size, and $W(\varepsilon^0, I)$ stands for the strain energy of an RVE when the partition is by the smallest window whose size is of a single fiber. This corresponds to the assumption

Voigt used, i.e., that the strain is uniform everywhere in the material. This is why we denote $W(\epsilon^0, I)$ by W^V . The volume averaging form, or strain energy density satisfies

$$w(\epsilon^0, \Delta) \leq w(\epsilon^0, \delta) \leq w(\epsilon^0, \delta') \leq w(\epsilon^0, I) \equiv w^V \quad \text{for} \quad I < \delta' < \delta < \Delta \quad (3.17)$$

Next let us introduce two traction boundary conditions on $B_\delta(\omega)$: unrestricted

$$t_i = \sigma_{ij}^0 n_j \quad x \in \partial B_\delta \quad (3.18)$$

and: restricted

$$t_i^r = \sigma_{ij}^0 n_j \quad x \in \partial B_\delta^s, \quad s = 1, 2, \dots, n^2 \quad (3.19)$$

The principle of minimum complementary energy states that, for the real field $\sigma(x)$ solution of the problem, the functional

$$\Pi^*(\tilde{\sigma}) = \int w^*(\tilde{\sigma}) dV - \int_{\partial B_\delta^d} t_i u_i dS \quad (3.20)$$

is a minimum among the values it takes for every stress field $\tilde{\sigma}(x)$ in B_δ that is admissible.

Because $\partial B_\delta = \partial B_\delta^t$ and $\partial B_\delta^d = \emptyset$, the potential energies $\Pi^*(\omega)$ and $\Pi^{*r}(\omega)$ (i.e., unrestricted versus restricted conditions) stored in B_δ under conditions (3.18) and (3.19), respectively, are

$$\Pi^*(\omega) = W^*(\omega; \sigma^0) \quad \text{and} \quad \Pi^{*r}(\omega) = W^{*r}(\omega; \sigma^0) \quad (3.21)$$

where

$$W^*(\omega; \sigma^0) = \int w^* dV \quad \text{and} \quad W^{*r}(\omega; \sigma^0) = \int w^{*r} dV \quad (3.22)$$

The principle of minimum complementary energy implies that, the complementary energies $\Pi^*(\omega)$ and $\Pi^{*r}(\omega)$ stored in $B_\delta(\omega)$ under conditions (3.18) and (3.19), respectively, satisfy the inequality

$$\Pi^*(\omega; \sigma^0) \leq \Pi^{*r}(\omega; \sigma^0) \quad (3.23)$$

or

$$W^*(\omega; \sigma^0) \leq W^{*r}(\omega; \sigma^0) \quad (3.24)$$

If we denote $W^*(\sigma^0, \delta)$ as the complementary energy of an RVE with partition by windows of size δ under traction controlled boundary condition, then from (3.24)

$$W^*(\sigma^0, \Delta) \leq W^*(\sigma^0, \delta) \leq W^*(\sigma^0, \delta') \leq W^*(\sigma^0, l) \equiv W^{*R} \quad \text{for } l < \delta' < \delta < \Delta \quad (3.25)$$

$W^*(\sigma^0, l)$ stands for the complementary strain energy of the RVE when the partition is by the smallest window whose size is of single fiber. This corresponds to the assumption Reuss used, i.e., the stress is uniform everywhere in the material. This is why we denote $W^*(\sigma^0, l)$ as W^{*R} .

The volume averaging form, or complementary energy density satisfies

$$w^*(\sigma^0, \Delta) \leq w^*(\sigma^0, \delta) \leq w^*(\sigma^0, \delta') \leq w^*(\sigma^0, l) \equiv w^{*R} \quad \text{for } l < \delta' < \delta < \Delta \quad (3.26)$$

Because the composite is ergodic, eqs. (3.17) and (3.26) can also be interpreted as the hierarchy structure in ensemble average sense

$$\langle w(\varepsilon^0, \Delta) \rangle \leq \langle w(\varepsilon^0, \delta) \rangle \leq \langle w(\varepsilon^0, \delta') \rangle \leq \langle w(\varepsilon^0, l) \rangle \equiv w^v \quad \text{for } l < \delta' < \delta < \Delta \quad (3.27)$$

and

$$\langle w^*(\sigma^0, \Delta) \rangle \leq \langle w^*(\sigma^0, \delta) \rangle \leq \langle w^*(\sigma^0, \delta') \rangle \leq \langle w^*(\sigma^0, l) \rangle \equiv w^{*R} \quad \text{for } l < \delta' < \delta < \Delta \quad (3.28)$$

with $w(\varepsilon^0, \delta)$ and $w^*(\sigma^0, \delta)$ representing the quantity of an arbitrary window of size δ , which may be placed anywhere in the whole material domain of any random sample.

In the above equations, we use ε^0 and σ^0 instead of $\bar{\varepsilon}$ and $\bar{\sigma}$, because under kinematic boundary condition,

$$\bar{\varepsilon} = \varepsilon^0 \quad (3.29)$$

which is called a strain averaging theorem, and under traction boundary condition,

$$\bar{\sigma} = \sigma^0 \quad (3.30)$$

which is called a stress averaging theorem.

It must be pointed out that the hierarchy structures shown in eqs. (3.27) and (3.28) are only proved for $\delta = n\delta'$; n is integer. We would like to generalize this inequality to an arbitrary pair of meso-scale windows with $\delta' < \delta$. This generalization can be done by the method of contradiction such as that in (Ostoja-Starzewski, 1999a), which is for a linear elastic composite. Because the proof procedure there is quite general, it can be used here without major modification. We will not repeat the proof here.

Even though (3.27) and (3.28) are proved for nonlinear elastic composites, based upon the argument at the beginning of this section, they can be used as guidelines in the elastoplastic response analysis.

When the material property of phase (one or both) is nonlinear elastic in a particular form as that in Kröner (1994), i.e.,

$$\sigma = \sum_{n=1} C_n \varepsilon^n, \quad \varepsilon = \sum_{n=1} S_n \sigma^n \quad (3.31)$$

where C_n and S_n represent the n th order elastic constants, the corresponding strain energy density and complementary energy density, respectively, are

$$w = \sum_{n=1} C_n \frac{\varepsilon^{n+1}}{n+1}, \quad w^* = \sum_{n=1} S_n \frac{\sigma^{n+1}}{n+1} \quad (3.32)$$

It is reasonable to assume the energy forms of the window in eqs. (3.27) and (3.28) to be

$$\langle w(\varepsilon^0, \delta) \rangle = \sum_{n=1} C_{n,\delta}^d \frac{(\varepsilon^0)^{n+1}}{n+1}, \quad \langle w^*(\sigma^0, \delta) \rangle = \sum_{n=1} (S_{n,\delta}^t) \frac{(\sigma^0)^{n+1}}{n+1} \quad (3.33)$$

for apparent properties, and

$$w(\varepsilon^0, \Delta) = \sum_{n=1} C_n^{eff} \frac{(\varepsilon^0)^{n+1}}{n+1}, \quad w(\sigma^0, \Delta) = \sum_{n=1} S_n^{eff} \frac{(\sigma^0)^{n+1}}{n+1} \quad (3.34)$$

for effective properties. Superscripts d and t indicate the associated boundary conditions are displacement and traction controlled boundary conditions, respectively. Because ε^0 and σ^0 are arbitrary, substitution of eqs. (3.33) and (3.34) into eqs. (3.27) and (3.28) yields

$$C_n^V \equiv \langle C_{n,l}^d \rangle \geq \langle C_{n,\delta'}^d \rangle \geq \langle C_{n,\delta}^d \rangle \geq C_n^{eff}, \quad \forall \delta' < \delta, n = 1, 2, \dots \quad (3.35)$$

$$S_n^R \equiv \langle S_{n,l}^t \rangle \geq \langle S_{n,\delta'}^t \rangle \geq \langle S_{n,\delta}^t \rangle \geq S_n^{eff}, \quad \forall \delta' < \delta, n = 1, 2, \dots \quad (3.36)$$

which are the structures obtained by Hazanov (1999). The comparison of tensors is understood in terms of quadratic forms. This means that, for two fourth rank tensors C and D , the assumption $C \geq D$ implies that

$$(C - D) : a : a \geq 0 \quad \text{for any tensor} \quad a_{ij} \neq 0 \quad (3.37)$$

When the material is linear elastic, we have

$$w(\varepsilon^0, \delta) = \frac{1}{2} \varepsilon^0 : C_\delta^d : \varepsilon^0, \quad w^*(\sigma^0, \delta) = \frac{1}{2} \sigma^0 : S_\delta^t : \sigma^0 \quad (3.38)$$

for apparent properties, and

$$w(\varepsilon^0, \Delta) = \frac{1}{2} \varepsilon^0 : C^{eff} : \varepsilon^0, \quad w^*(\sigma^0, \Delta) = \frac{1}{2} \sigma^0 : S^{eff} : \sigma^0 \quad (3.39)$$

for effective properties. Because of $(S^{eff})^{-1} = C^{eff}$, eqs. (3.27) and (3.28) can be reduced to

$$C^R \equiv (S^R)^{-1} \equiv \langle S_l^t \rangle^{-1} \leq \langle S_{\delta'}^t \rangle^{-1} \leq \langle S_\delta^t \rangle^{-1} \leq C^{eff} \leq \langle C_\delta^d \rangle \leq \langle C_{\delta'}^d \rangle \leq \langle C_l^d \rangle \equiv C^V, \quad \forall \delta' < \delta \quad (3.40)$$

which is the structure obtained in Huet (1990) and Ostoja-Starzewski (1993).

Inequalities (3.27) and (3.28) are proved in potential forms. Next, Following Hill (1983), we restrict our attention to existing strain and stress state in which increments of plastic strain are constrained to be of order $1/E \times$ the stress increments. Let $(d\sigma_{ij}, d\varepsilon_{ij})$ be the actual increments

of stress and strain produced by given external stress increments dt_i over ∂B_δ , or by given external kinematic increments over ∂B_δ .

We define the incremental modulus under displacement boundary condition through

$$\overline{d\sigma} = C_\delta^{Td} : \overline{d\varepsilon} = C_\delta^{Td} : d\varepsilon^0 \quad (3.41)$$

and incremental compliance under traction boundary condition through

$$\overline{d\varepsilon} = S_\delta^{Tt} : \overline{d\sigma} = S_\delta^{Tt} : d\sigma^0 \quad (3.42)$$

Again, superscript ‘ d ’ and ‘ t ’ indicates that the quantity is obtained under kinematic and traction boundary conditions, respectively. Superscript ‘ T ’ indicates the associated tangent quantity.

Here without proof, we conjecture that, in elastoplastic problem, for work hardening composites, under monotonically proportional loading, there is a hierarchy of bounds on the effective tangent stiffness tensor C^{Teff}

$$C^{TS} \equiv (S^{TS})^{-1} = \langle S_I^{Tt} \rangle^{-1} \leq \langle S_\delta^{Tt} \rangle^{-1} \leq \langle S_\delta^{Tt} \rangle^{-1} \leq (S^{Teff})^{-1} = C^{Teff} \leq \langle C_\delta^{Td} \rangle \leq \langle C_\delta^{Td} \rangle \leq \langle C_I^{Td} \rangle \equiv C^{TT} \quad \forall \delta' < \delta \quad (3.43)$$

where C_I^{Td} is obtained when $\delta = l$ (size of a single fiber) under the assumption Taylor used (1938), i.e., the strain rate is uniform everywhere in the material. This is why we denote $\langle C_I^{Td} \rangle$ by C^{TT} ; S_I^{Tt} is obtained when $\delta = l$ under the assumption Sachs (1928) used, i.e., the strain is uniform everywhere in the material. This is why we denote $\langle S_I^{Tt} \rangle$ by S^{TS} . In (3.44), the first superscript of each quantity is T , which indicates tangent modulus, as has been defined previously.

The linear apparent elastic property under mixed boundary condition (3.5) was discussed in (Hazanov and Huet, 1994; Hazanov and Armieur, 1995). They proved that the apparent moduli under mixed boundary conditions are bounded by those obtained under displacement controlled

and traction controlled boundary conditions. The mixed boundary value problem is very complicated. In the next section, we choose a special mixed boundary loading, under which we investigate the elastoplastic response.

4. ELASTOPLASTICITY OF A FIBER-REINFORCED COMPOSITE

4.1. Material model

Considerable attention has been paid to the modeling of metal-matrix composites (MMC) which are made of a ductile metallic matrix with embedded high strength ceramic reinforcements such as continuous fibers, whiskers or particles. Since the MMC possess a combination of properties such as low density, high strength, stiffness, creep and wear resistance, they are appropriate candidates for aerospace and automotive applications. Under longitudinal loading (i.e., in the fiber direction) continuous fiber reinforced MMC have demonstrated an excellent performance. In this case the material makes full use of high strength fibers. However, the continuous fiber reinforced MMC are somewhat limited due to their relatively poor transverse properties, and this is what we focus on in the numerical example to follow.

More specifically, we consider a composite material behavior, which is a special case of relation (2.1): it has the same elastic constants (Young's Moduli E and Poisson ratio ν) for both matrix and fiber, and the fiber-matrix interface is perfectly bonded. Both phases are isotropic, and fibers are linear elastic while matrix is elastoplastic. We take $p = 1$ to denote the matrix, and $p = 2$ to denote the inclusion material.

For the matrix, the von Mises yield criterion is used, and the rate-independent plasticity with associated flow rule and isotropic hardening is assumed. The matrix' stress-strain curve is characterized by a piece-wise power-law (e.g., Dowling, 1993)

$$\frac{\sigma}{\sigma_0} = \begin{cases} \varepsilon/\varepsilon_0, & \text{if } \varepsilon \leq \varepsilon_0 \\ (\varepsilon/\varepsilon_0)^N, & \text{else} \end{cases} \quad (4.1)$$

with yield stress $\sigma_0 = E\varepsilon_0$, and ε_0 is the yield strain. When $N = 0$, the material is perfectly plastic, and when $N = 1$, the material is linearly elastic.

4.2. Numerical results

We assume plane strain deformation and use small deformation theory. Our material is homogeneous before yielding and the response is linear elastic under applied loading (3.3), (3.4) or (3.5). Also prior to yielding, the stress and strain in the material are uniform and equal to the applied loading for each type of boundary condition applied. In the analysis we apply pure shear loading through boundary conditions:

displacement: $\varepsilon_{xx}^0 = -\varepsilon_{yy}^0 = \varepsilon$, $\varepsilon_{xy}^0 = 0$;

traction: $\sigma_{xx}^0 = -\sigma_{yy}^0 = \sigma$, $\sigma_{xy}^0 = 0$;

mixed: $\varepsilon_{xx}^0 = -\varepsilon_{yy}^0 = \varepsilon$, $\sigma_{xy}^0 = 0$.

The material constants are: $\varepsilon_0 = 1/300$, $\sigma_0 = 170\text{MPa}$, $N = 0.1$, $E = \sigma_0/\varepsilon_0 = 51\text{GPa}$, $\nu = 0.3$. Volume fraction of fiber is chosen to be 0.35. We take the window sizes to be $\delta = 6$ and 20, with examples for these two sizes shown in Fig. 1. The finite element analysis is done by ABAQUS 5.5 (Hibbit, Karlson, Sorensen, Inc., 1995) was carried out on 8 and 4 realizations $B(\omega)$ of the composite for $\delta = 6$ and $\delta = 20$, respectively.

In Fig. 2 and Fig. 3, the equivalent plastic strain (PEEQ) contour plots are given. Under kinematic boundary condition and mixed boundary condition, the applied strain in the x direction

is 15 times the yield strain ε_0 , while under traction boundary condition, the applied stress in the x direction is the same as the yield stress σ_0 . We can find that directions of shear bands are at 45° approximately, which is understandable, because we applied bi-directional loading with equal amplitude in both directions, and before yielding the material was homogeneous. After yielding, however, the material becomes inhomogeneous, so the shear bands will not be at 45° direction exactly.

The patterns of equivalent plastic strain fields, especially shear bands, under the three boundary conditions are different. Comparison between the shear band patterns under different boundary conditions shows that the uniform distribution of shear bands ranks in the following order in terms of boundary conditions: displacement, mixed, traction. Correspondingly, the response curves under different boundary conditions rank in the same order in terms of hardening effect (see Figs. 4, 5 and 6). Under traction boundary condition, the plastic deformation takes place via the weakest regions, and also because shear band formation is such a local process that, even though there are some possible paths for new shear bands to form, only several shear bands dominate the whole elastoplastic deformation process. When the boundary condition is displacement controlled, the main parts of shear bands are constrained within the window (see the bright colored parts of shear bands). This is another reason why the response curves under displacement condition are higher than those under traction boundary condition. The shear band pattern under mixed boundary condition is similar to that under displacement condition. However, under mixed condition, major plastic deformation is along several shear bands, i.e., more localized than that under displacement one, while this localization is not as strong as that under traction boundary condition. This explains that response curve under mixed condition is bounded by those under displacement and traction conditions.

As the window size increases, due to the random distribution of fibers, it becomes difficult for a shear band to find a path through entire window under traction boundary conditions. While both Figs 2(c) and 3(c) show that dominating shear bands tend to form at the window corners, this ‘corner effect’ decreases with the window size going up. In fact, the pattern of shear bands under different conditions is much more alike at large than at small windows, and this illustrates the tendency to homogenize with δ going to infinity. As expected, this is paralleled by the decreasing effects of boundary conditions on the response curves displayed in the next figures that are discussed below.

A related investigation, employing periodic boundary conditions on a periodic random composite, was carried out by Moulinec and Suquet (1998), wherein the matrix material was perfectly-plastic. The plastic flow of the material occurred through infinitesimally thin slip-lines, to which our finite-thickness shear bands would tend to in the limit of perfect plasticity (Suquet, 2000).

In Fig. 4 to Fig. 5, we plot the relationship between average stress and average strain in x direction for each sample. It can be observed that crossing happens between response of different random samples. We also observed that the scatter of response curves under displacement condition is larger than that under mixed condition, and the scatter under traction is the smallest. The scatter of $\delta = 20$ is smaller than that of $\delta = 6$. Since, prior to yielding, the material is homogeneous, there are common yielding stress and strain for all random samples under different boundary conditions.

The final comparison is made in Fig. 6. Plotted here are the ensemble average responses under displacement and traction boundary conditions for $\delta = 6$ and $\delta = 20$, as well as those from the Taylor and Sachs bounds. It can be seen that, in accordance with (3.27) and (3.28), as

the window size increases, the elastoplastic bounds under displacement and traction boundary conditions become even tighter. As expected, Taylor and Sachs provide broadest possible bounds. These bounds not only bound the true effective response, but also bound the response under mixed boundary condition. From Fig. 6, we see that the rates of average response curves, i.e., the tangent moduli, satisfies the conjecture (3.43).

5. CLOSING REMARKS

We introduced scale-dependent bounds on the effective instantaneous moduli of elastoplastic random composite materials with an associated flow rule. These are upper and lower bounds obtained from uniform displacement and traction boundary conditions applied to finite size domains. We find that, similar to the elastic case, our bounds become tighter with the increasing window size. For small window sizes, displacement conditions yield to rather uniform patterns of shear bands, while traction conditions lead to highly localized ones. Indeed, the approach to the homogenization limit is paralleled by the ever more uniform shear band fields. At the same time, the scatter of response curves decreases. Further more, the present study may be useful in the research on stability and bifurcation phenomenon in dissipative heterogeneous materials.

The determination of the rate of approach to the classical RVE in random microstructures is of interest not only in micromechanics. Consider, for example, the finite element and difference methods employed in solution of arbitrary boundary value problems of solid mechanics. These methods are typically deterministic in that they tacitly assume that any single finite element (or difference) volume is at least the size of the RVE. However, as the mismatch in material properties on the microscale increases, the approach to the classical RVE in linear

elasticity may be very slow (e.g., Ostoja-Starzewski, 1998) and the finite element is no longer described by a deterministic Hooke's law. The finite element plays the role of a mesoscale window, and the bounds stemming from displacement and traction boundary conditions allow establishment of bounds on the global response (Ostoja-Starzewski, 1999b).

A related situation was recognized in the solution of boundary value problems of heterogeneous, perfectly-plastic solids (Ostoja-Starzewski and Ilies, 1996). Choice of a finite difference mesh led to the treatment of the yield condition as a random field with variability on the scale of a single finite difference cell. However, no micromechanically based information on that field was available at the time. We believe this paper is a step in that direction.

ACKNOWLEDGEMENT

We benefited from comments of P. Suquet and an anonymous reviewer. Support by the NSF under grants CMS-9713764 and CMS-9753075 is gratefully acknowledged.

References

- Accorsi, M.L. and Nemat-Nasser, S., 1986. Bounds on the overall elastic and instantaneous elastoplastic moduli of periodic composite, *Mech. Mater.* **5**, 209-220.
- Brockenbrough, J.R., Suresh, S. and Wienecke, H.A., 1991. Deformation of metal-matrix composites with continuous fibers: geometrical effects of fiber distribution and shape, *Acta Metall. Mater.* **39**, 735-752.
- Dowling, N. E., 1993. *Mechanical Behavior of Materials: Engineering Methods for Deformation, Fracture, and Fatigue*, Englewood Cliffs, N.J.: Prentice Hall.
- Hazanov, S., 1998. Hill condition and overall properties of composites, *Arch. Appl. Mech.* **68**, 385-394.
- Hazanov, S., 1999. On apparent properties of nonlinear heterogeneous bodies smaller than the representative volume, *Acta Mechanica*, **134**, 123-134.
- Hazanov, S. and Huet, C., 1994. Order relationships for boundary conditions effect in the heterogeneous bodies smaller than the representative volume, *J. Mech. Phys. Solids* **42**, 1995-2011.
- Hazanov, S. and Amieur, M., 1995. On overall properties of elastic heterogeneous bodies smaller than the representative volume, *Int. J. Engng. Sci.* **23**, 1289-1301.
- Hibbit, Karlson, Sorensen, Inc., 1995. 1080 Main Street, Pawtucket, RI, USA, *ABAQUS User's Manual Version 5.5*.
- Hill, R., 1963. Elastic properties of reinforced solids: some theoretical principles, *J. Mech. Phys. Solids* **11**, 357-372.
- Hill, R., 1983. *The Mathematical Theory of Plasticity*, Clarendon Press, Oxford.
- Huet, C., 1981. Remarques sur la procédure d'assimilation d'un matériau hétérogène à un milieu continu équivalent. In C. Huet and A. Zaoui (Eds.), *Rheological Behaviour and Structure of Materials*, Presses de l'ENPC, Paris, 231-245.
- Huet, C., 1982. Universal conditions for assimilation of a heterogeneous material to an effective medium, *Mech. Res. Comm.*, **9**, 165-170.
- Huet, C., 1984. On the definition and experimental determination of effective constitutive equations for heterogeneous materials, *Mech. Res. Comm.*, **11**, 195-200.
- Huet, C., 1990. Application of variational concepts to size effects in elastic heterogeneous bodies, *J. Mech. Phys. Solids* **38**, 813-841.

- Li, G. and Ponte Castañeda, P. 1994. Variational estimates for the elastoplastic response of particle-reinforced metal-matrix composites, *Appl. Mech. Rev.* **47**(1, Pt. 2), 577-594.
- Moulinec, H., and Suquet, P., 1994. A fast numerical method for computing the linear and nonlinear mechanical properties of composites, *C.R. Acad. Sci. Paris*, **318**, Série II, 1417-1423.
- Moulinec, H., and Suquet, P., 1998. A numerical method for computing the overall response of nonlinear composites with complex microstructure, *Comput. Methods Appl. Mech. Engng.*, **157**, 69-94.
- Ostoja-Starzewski, M., 1993. Micromechanics as a basis of random elastic continuum approximations, *Probabilistic Eng. Mech.* **8**, 107-114.
- Ostoja-Starzewski, M., 1998. Random field models of heterogeneous materials, *Intl. J. Solids Struct.* **35**(19), 2429-2455.
- Ostoja-Starzewski, M., 1999a. Scale effects in materials with random distributions of needles and cracks, *Mech. Mater.*, **31**, 883-893.
- Ostoja-Starzewski, M., 1999b. Microstructural disorder, mesoscale finite elements, and macroscopic response, *Proc. R. Soc. Lond. A*, **455**, 3189-3199.
- Ostoja-Starzewski, M., and Ilies, H. 1996. The Cauchy and characteristic boundary value problems of random rigid-perfectly plastic media, *Intl. J. Solids Struct.* **33**(8), 1119-1136.
- Ponte Castañeda, P. 1992. New variational principles in plasticity and their application to composite materials, *J. Mech. Phys. Solids* **40**, 1757-1788.
- Ponte Castañeda, P. and Suquet, P., 1998. Nonlinear composite, *Advances in Applied Mechanics*, **34**, 171-302.
- Sab, K., 1992. On the homogenization and the simulation of random materials, *Eur. J. Mech. A/Solids* **11**, 585-607.
- Sachs, G., Zur Ableitung einer Fließbedingung, 1928. *Z. Ver. Deutsch. Ing.* **72**, 734-736.
- Sanchez-Palencia, E and Zaoui, A., 1987. *Homogenization Techniques for Composite Media*, Lecture Notes in Physics **272**, Springer-Verlag.
- Shen, Y., Finot, M., Needleman, A. and Suresh S., 1995. Effective plastic response of two-phase composites, *Acta Metall. Mater.* **43**, 1701-1722.
- Stoyan, D., Kendall, W.S and Mecke, J., 1987. *Stochastic Geometry and its Application*, John Wiley & Sons.
- Suquet, P., 2000. *Private Communication*.

- Talbot, D.R.S. and Willis, J.R., 1998. Upper and lower bounds for the overall response of an elastoplastic composite, *Mech. Mater.* **28**, 1-8.
- Taylor, G. I., Plastic strain in metals, 1938. *J. Inst. Met.* **62**, 307-324.
- Teply, J.L. and Dvorak, G.J, 1988. Bounds on the overall instantaneous properties of elastic-plastic composites, *J. Mech. Phys. Solids* **45**, 87-111.
- Werwer, M., Cornec, A. and Schwalbe, K.-H., 1998. Local strain fields and global plastic response of continuous fiber reinforced metal-matrix composites under transverse loading, *Comput. Mater. Sci.* **12**, 124-136.
- Willis, J.R. and Talbot, D.R.S., 1990. Variational methods in the theory of random composite material, in *Continuum Models and Discrete Systems* **1**, 113-131.

FIGURE CAPTIONS

Fig. 1 – Window sample: (a) $\delta = 6$; (b) $\delta = 20$

Fig. 2 – Contour plot of equivalent plastic strain for window shown in Fig. 1 (a) under different boundary conditions: (a) displacement controlled (b) mixed (c) traction controlled

Fig. 3 – Contour plot of equivalent plastic strain for window shown in Fig. 1 (b) under different boundary conditions: (a) displacement controlled (b) mixed (c) traction controlled

Fig. 4 – Responses of eight sample windows for $\delta = 6$ under different boundary conditions: displacement controlled (dotted lines), mixed (solid lines) and traction controlled (dashed lines)

Fig. 5 – Responses of four sample windows for $\delta = 20$ under different boundary conditions: displacement controlled (dotted lines), mixed (solid lines) and traction controlled (dashed lines)

Fig. 6 – Ensemble average responses under different boundary conditions and four other curves

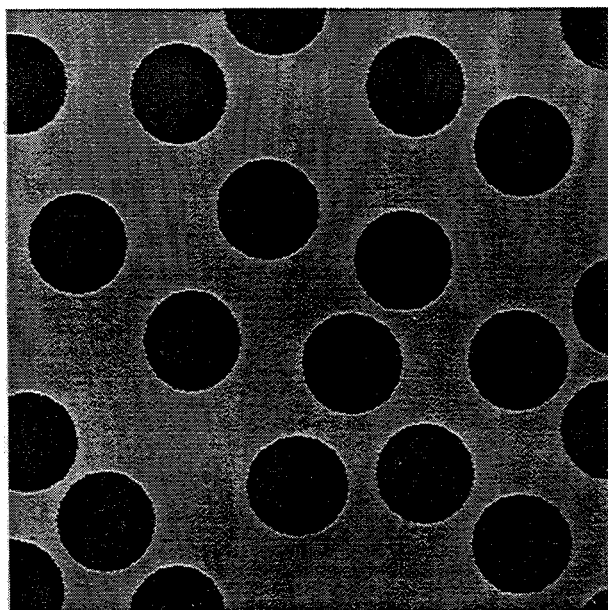


Figure 1a: Micrograph of a material with large circular pores.

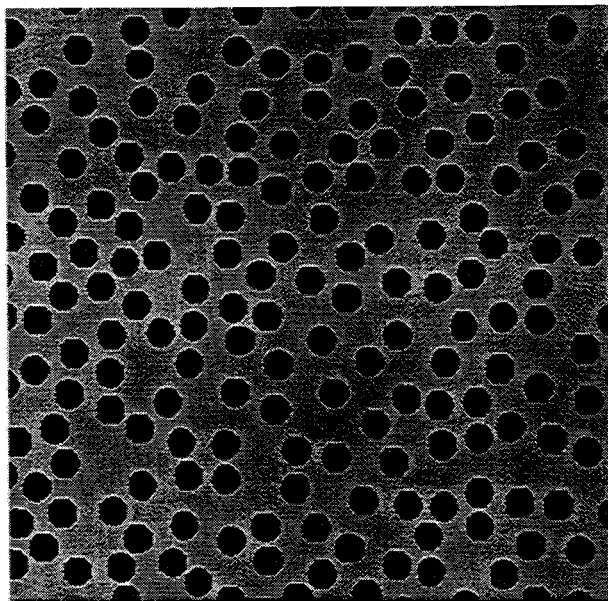
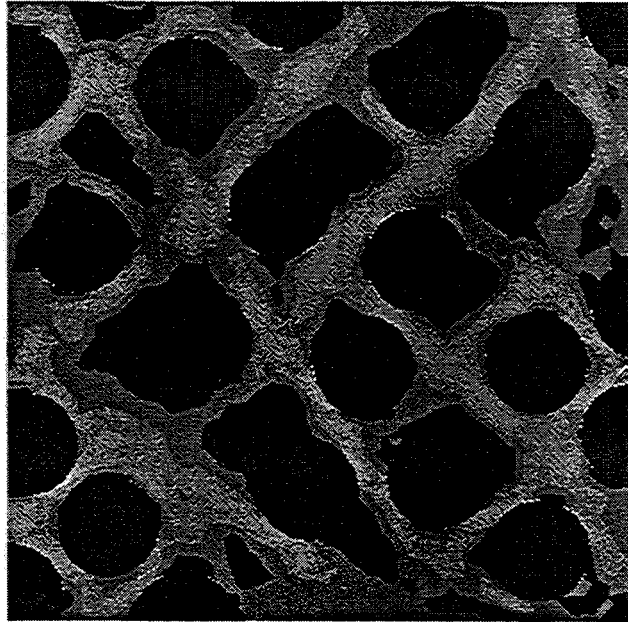
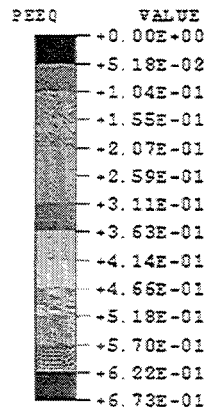
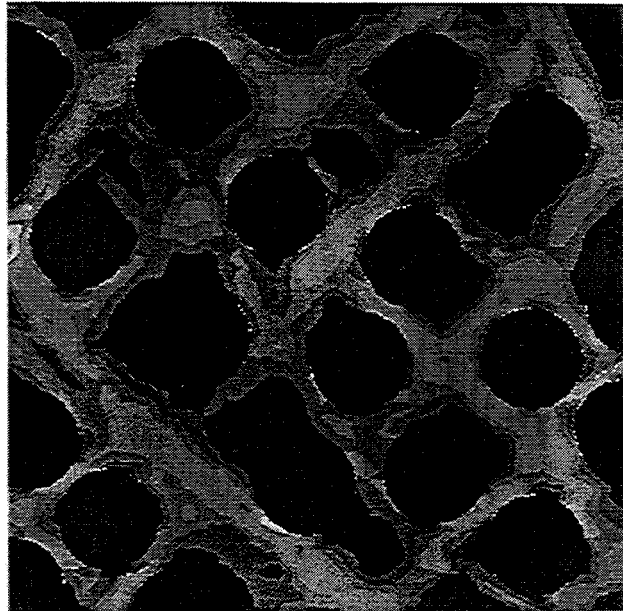
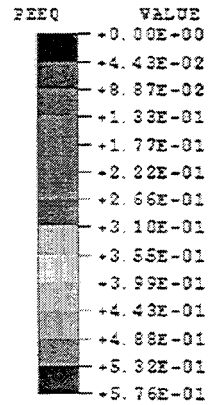


Figure 1b: Micrograph of a material with small circular pores.

Figure 1



(a)



(b)

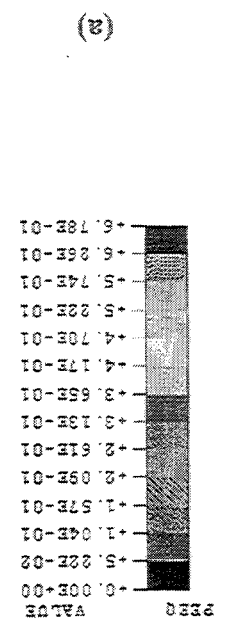
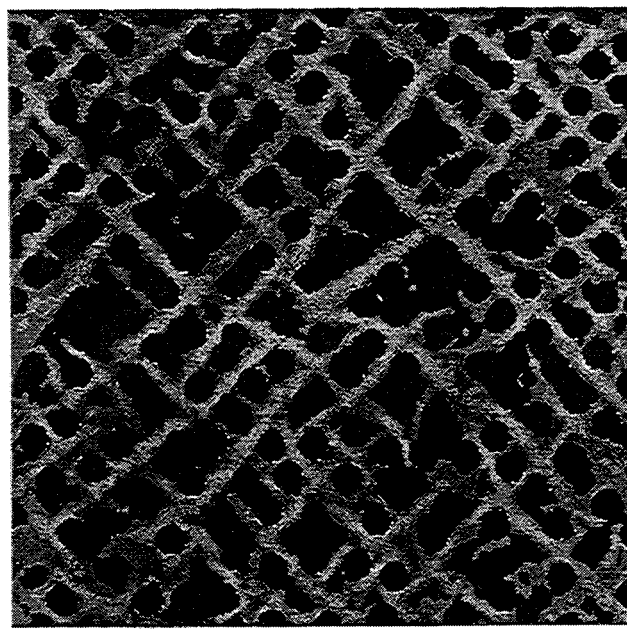


Figure 2

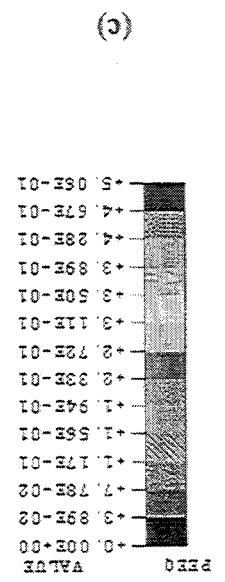
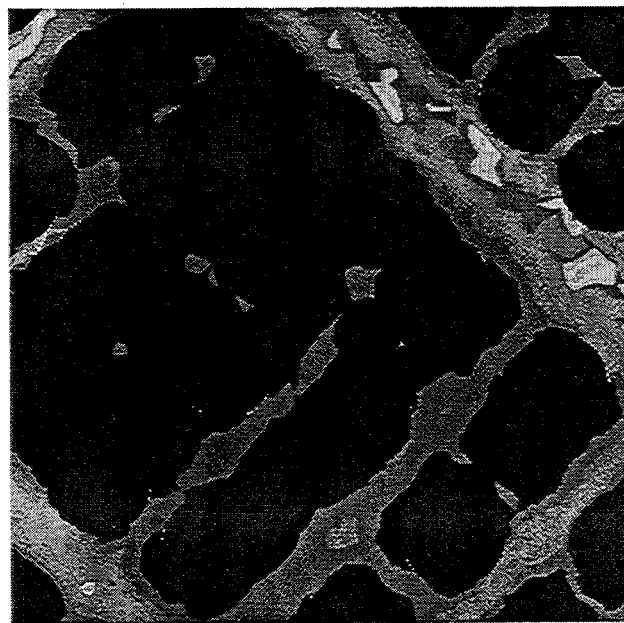
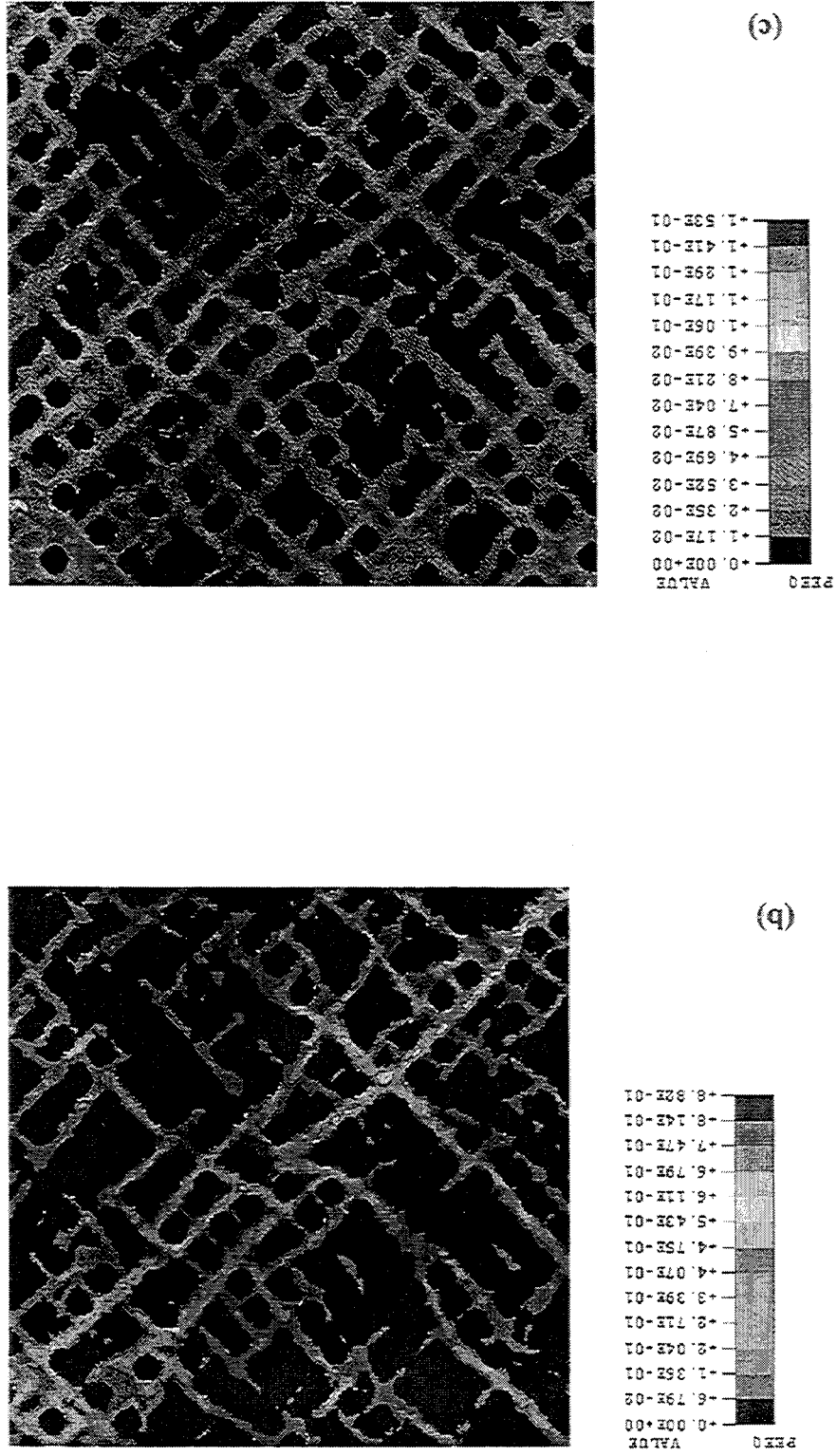


Figure 3



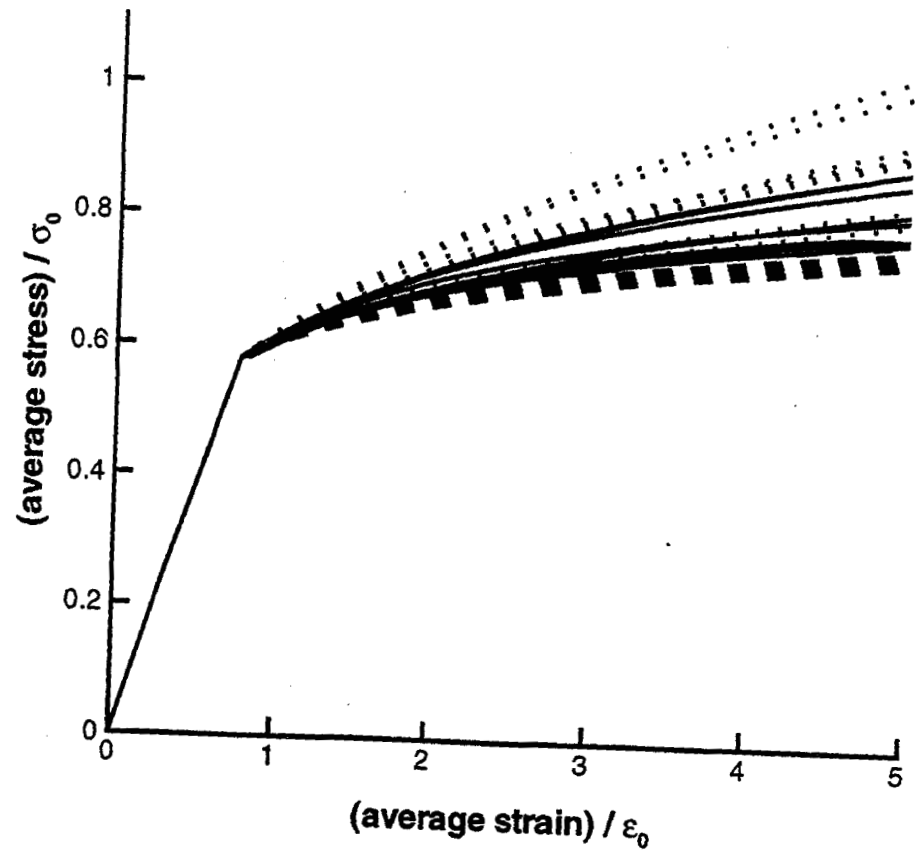


Figure 4

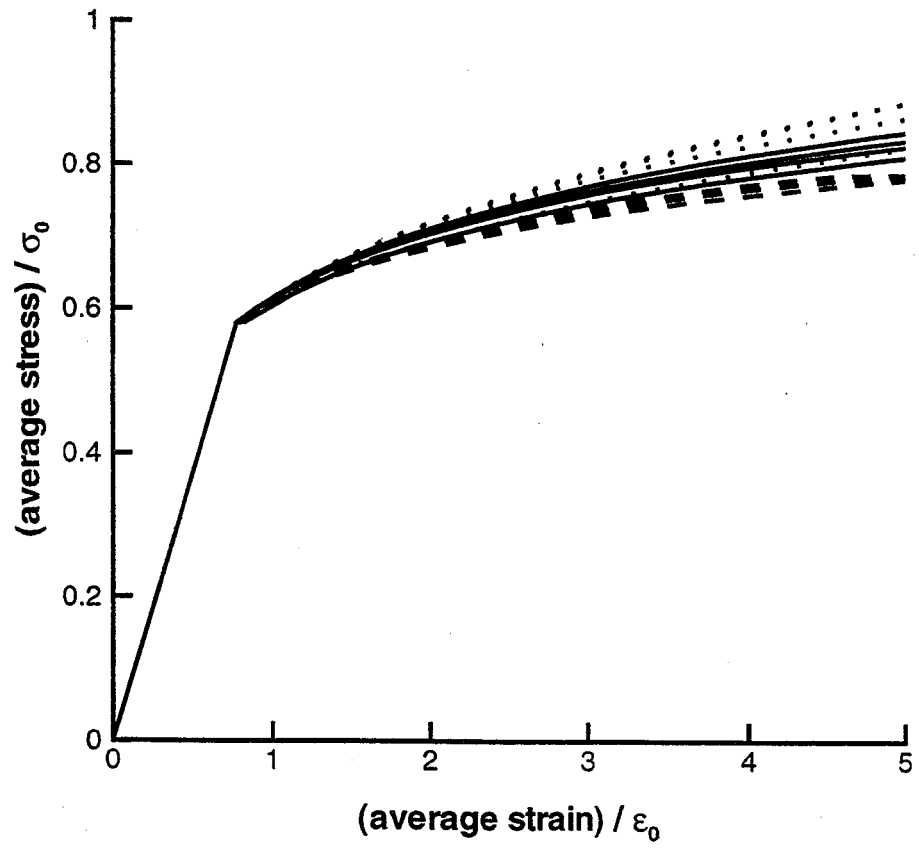


Figure 5

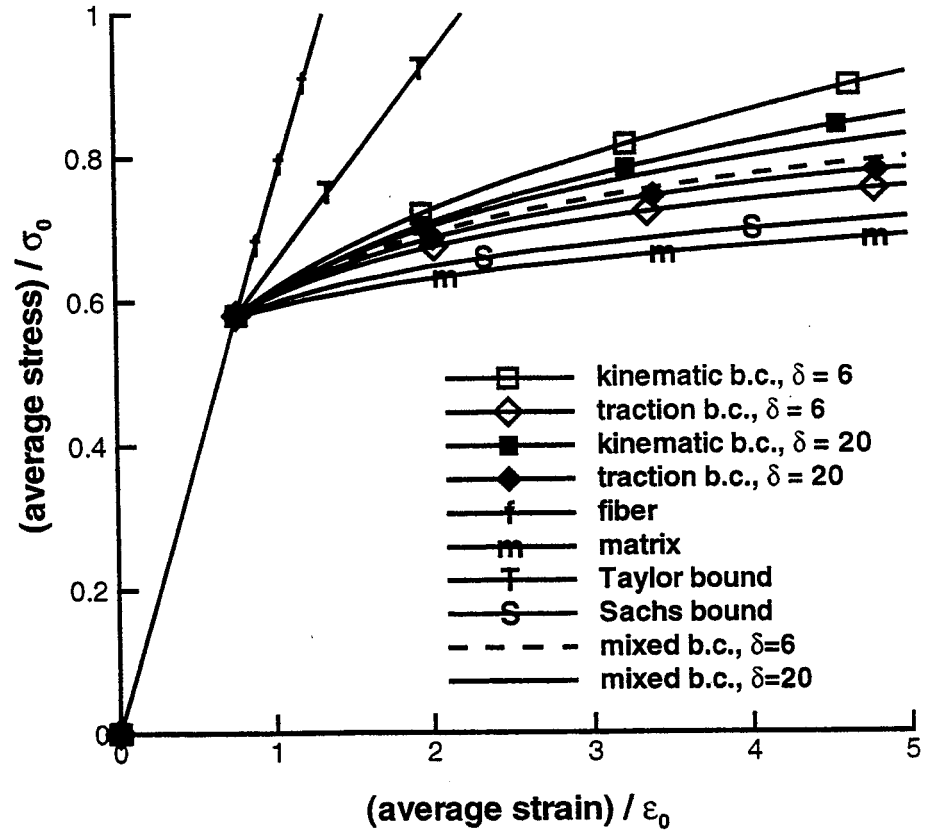


Figure 6